Clays as indicators of paleoclimate and source rocks in The Chu-Sarysu Basin (Kazakhstan)

Askar Munara, Michel Cathelineau, Cedric Carpentier, Nadir Abylay

CLAYS AS INDICATORS OF PALEOCLIMATE AND SOURCE ROCKS IN THE CHU-SARYSU BASIN (KAZAKHSTAN)

A. Munara*, M. Cathelineau*, C. Carpentier*, N. Abylay

* UMR GeoRessources, Université de Lorraine, CNRS, CREGU, 54500, Nancy, France

Abstract

Newly formed smectite and palygorskite and their association are good proxies of a subtropical climate alternating dry and warm/ humid seasons during the late Cretaceous during the formation of the Chu-Syrasu basin. The association of fine-grain clays, smectite and fibres (palygorskite) and the occurrence locally of grains of albite, and natrolite, indicate they formed from water, slightly alkali-rich, and enriched in silica and magnesium. These clays may result partly from the alteration of volcanic rocks (glass) either in situ in case of volcanic emissions during sedimentation or close as smectite are euhedral and palygorskite well preserved. The flood plain may have been submitted during the hot season to drying, favouring the formation of brines which interacted with volcanic glass. Evaporation processes could have thus triggered the oversaturation with respect to smectite and palygorskite.

Besides, muscovite as coarse grain particles, illite and chloritized biotites attest to a second source compatible with the coarse grain microcline and quartz, which can derive from granites. Source rocks could be, therefore, dual, with acid plutonic series (peraluminous granites probably) releasing coarse-grained detrital phyllosilicates (muscovite and biotite-chlorite) transported together with quartz and feldspars by rivers, and volcanic series, altered into newly-formed clays (smectite and palygorskite).

1- Introduction

Clay minerals are the main constituent of shales and a minor component of sands in the fluvial sediments of the Chu-Syrasu basin (Kazakhstan). Shales and sands alternate in the basin, and clays may be considered good indicators of the provenance of the detrital minerals as well as markers of the alteration conditions in the weathering. These clays may have formed or evolved during sedimentation or early post-sedimentation stages. However, the temperature developed in the basin is relatively low due to a thin overburden of less than one kilometre and not favourable to profound alteration of the clays.

The nature of clays within the sands and the layers rich in clay is essential to determine at different scales, from the horizons at the drilling scale to the basin scale. Clays' lateral and vertical distribution between the four main formations (Kanjugan, Uyuk, Ikansk, and Intymak) remains incompletely determined. As clay mineralogy can reflect either some diagenetic processes, the source of detrital minerals or the influence of U-mineralization processes, it was

characterised by representative samples from the four sedimentary formations, thanks to samples from drill cores from the South-Central Muyumkum and Tortkuduk areas provided by Katco company. The nature of the clays is also essential to determine as it can represent a penalising phase for the mining operation during in situ recovery.

2-Material and methods

a-Geology

The study of clay material was carried out on existing drilling cores from the Southern and Central Moiynkum and Tortkuduk deposits within four sedimentary formations thanks to collaborative works with Areva (now Orano) and Katco companies. Twenty-eight samples were selected from 13 wells of South, Central Muyunkum and Tortkuduk fields with the help of JV Katko LLP company.

The Chu-Sarysu Basin is about 200 kilometres wide (east-west) and 800 kilometres long (north-south), separated from the Syrdarya Basin by the Karatau Range (Bliachova et al., 1976, Bliachova and Shakhverdov,1984). The exploration in the Chu-Sarysu Basin, the first of which was undertaken in the late 1950s, led to the first explorations in the Chu-Sarysu Basin in the late 1950s and led to the discovery of numerous deposits: Inkai, Uvanas, Muyunkum, Mynkuduk, Akdala, Jalpak (Shakhverdov,1988). The Meso-Cenozoic formations are unconformable with the Paleozoic basement and have various lithologies: alternating sands, clays, silts, gravels, pebbles and limestones. Uranium mineralisation is mainly in roll-front deposits located in several stratigraphic horizons. The uranium, transported in solution under oxidising conditions, was precipitated by various reducing agents.

The Uyuk horizon is composed of shallow marine, littoral and deltaic facies. The horizon is divided into two zones: a lower sandy zone (mineralised zone) and an upper silty-clay zone mineralised zone) and an upper silty-clay zone. The depth of the upper zone is 395 to 525 metres in the southern part of the Suzak depression and 240 to 314 metres in the Tortkuduk area. The lower zone is composed of sands of varying grain sizes (medium and very fine grain) with little clay. The upper zone consists of clays, silts and clayey sands. The boundary between the lower and the upper part is a mixing zone between the upper part corresponds to a mixing zone between the sands of the lower horizon and the clays of the upper horizon. The boundary between the two zones is, therefore, irregular. The total thickness of the Uyuk horizon varies

between 30 metres in the Tortkuduk area and 80 metres in the deepest part of the Suzak depression.

The Ikansk horizon is divided into two sub-horizons: the lower part is represented by littoral and deltaic facies (medium to very fine-grained sands, well sorted) and the upper part by deltaic facies (coarser, poorly sorted sands with silty lenses). Clays and silts separate these sub-horizons over a thickness of 0.5 to 5 metres. In the Suzak depression, the thickness of the Ikansk horizon varies from 50 to 55 metres, and its depth is between 380 and 550 metres.

The Intymak horizon is characterised by a grey-green to black clay series, possibly mixed with black, Cretaceous volcanic ash. The thickness of the formation varies from 20 to 120 metres.

Petrographic observations and chemical analysis were performed on separated clay fractions of less than two μm. The samples were cleaned, dried, and degreased with acetone for one night. The clays were then separated by ultrasonic treatment of samples followed by ultracentrifugation.

b-Methods

X-Ray Diffraction (XRD): XRD data were collected with a D8 Bruker diffractometer with Co $K_\alpha 1$ radiation (λ=1.7902 Å). Diffractograms of non-oriented powders were obtained to identify non-clay minerals. XRD analysis was also carried out for the air-dried and ethylene glycol (EG) saturated oriented specimens of the < 2 μm fraction.

SEM micrographs were obtained using a Hitachi S-2500 Fevex scanning electron microscope using thin sections. Semi-quantitative chemical analyses were also performed. The separated < 2μm fraction of each run-sample was also observed to check the nature of newly formed non-clay minerals intimately associated with the coarse-grained phyllosilicates.

TEM image and Energy Dispersive Spectroscopy (EDS-TEM): Micro-chemical analyses of isolated clay particles of the < 2 μm fraction were obtained with an EDAX energy dispersive X-ray analyser attached to a CM20-Philips instrument operating at 200kV equipped with Si-Li detector and Li super ultra-thin windows SUTW. Spectra were collected under nanoprobe mode for 40 s from an area ~ 10 nm in diameter. Elemental composition was calculated assuming the thin film criteria (SMTF program: semi-quantitative metallurgical thin film program) and using k-factors calibrated with independently analysed macroscopic micas, with a maximum error of 5% for each element.

Electron microprobe analysis: The chemical composition of coarse-grained clay particles was obtained using electron microprobe analysis (EMA). Electron microprobe analyses (EMPA) of muscovite, biotite and Fe-chlorite were performed on representative thin sections at SCMEM (Nancy, France). Si, Al, Mg, Fe, Mn, K, V, Ti, Na, and Ca were analysed using a CAMECA SX100 instrument calibrated using natural and synthetic minerals or compounds such as albite (Si, Na), Al2O3 (Al), olivine (Mg), hematite (Fe), MnTiO3 (Mn), Co (Co), NiO (Ni). The analytical conditions were a current of 12 nA, an accelerating voltage of 15 kV and a counting time of 10 s. The analyses have a spatial resolution of 1 to 2 microns. Structural formulae were calculated arbitrarily based on 11 O per half unit cell, i.e. an $O_{10}(OH)_2$ base, and considering all iron as trivalent.

Table I. Main features of the studied samples

	Formation	Age	Borehole-Sample	Depth, m	Description
Tortkuduk Nord	Uyuk	Eocene	1722-109	275,7	Brown-greenish clay, compacted in oxidised sand
	Betpakdala	Miocene	1750-2	266,4	Grey-greenish clay homogeneous, compacted
	Intymak	Eocene	1750-9	270,4	Green sandy clay, fine sand, compacted, bivalve
	Intymak	Eocene	1750-12	273,1	Medium sand, pebbles of clays, grey-green
	Intymak	Eocene	1750-14	275,0	Greenish clay, compacted, intercalation medium sand
	Intymak	Eocene	1750-16	276,2	Light greenish clay, compacted, intercalated fine sand
	Uyuk	Eocene	1750-18	278,2	Brown-green clay, sandy
	Uyuk	Eocene	1750-19	278,9	Greenish-black clay, compacted, O.M.
	Uyuk	Eocene	1750-21	279,9	Brownish-black clay, fine-medium sand, intercalation
	Uyuk	Eocene	1750-24	281,8	Grey-greenish clay, fine, sandy
	Uyuk	Eocene	1750-45	304,3	Grey-greenish clay, compacted
	Uyuk	Eocene	1750-48	308,7	Yellow-brown clay, compacted-plastic, Py and O.M
	Uyuk	Eocene	1750-49	311,6	Black clay, oxidised, compacted, much debris
	Uyuk	Eocene	1750-50	314,8	Brownish-black compacted clay
	Uyuk	Eocene	1321-66	308,5	Greyish clay (compacted)
	Uyuk	Eocene	1321-70	317,1	Yellow clay(compacted)
	Betpakdala	Miocene	1319-83	270,3	Grey-greenish sandy clay (compacted)
Muyunkum Central	Uyuk	Eocene	642-2	334	White and green sand and clay; reduced area; medium, mineralised
	Uyuk	Eocene	421-5a, b	390,2	Carbonated sandy dark grey clay with O. M.: reduced; fine
	Intymak	Eocene	996-1	390,6	Dark grey black sand; reduced; medium fine
	Uyuk	Eocene	996-10	450,5	Black clay; reduced zone
	Uyuk	Eocene	998-7a, b	439,7	Dark grey clay, green: oxidised/reduced
	Uyuk	Eocene	1427-144	434,0	Grey-greenish clay with O.M. and sulphides
Muyunkum South	Uyuk	Eocene	781-6a-d	420,5	Grey and yellow sand black clay: middle-fine
	Ikansk	Eocene	781-2	392,2	Passage clay and white and green sand; oxidised/reduced
	Ikansk	Eocene	774-1a, b	253,4	White and yellow sand with clay: oxidised; medium fine
	Ikansk	Eocene	761-2	403,6	Dark grey sand with clay; reduced/mineralised; medium fine
	Uyuk	Eocene	768-4a-i	427,2	White sand with dark grey clay and medium, coarse, mineralised

3- Results

a-Clay mineralogy

Four main clay minerals were identified: smectite, illite, kaolinite and palygorskite. In addition, larger-size detrital phases are mixed with the fine-grained clays but frequently occur in the fine-grained fraction: muscovite and chlorite.

Smectite

Smectite is uniformly presented in all samples from Uyuk formation to the Miocene Betpakdala system in large amounts, smectite being the predominant mineral found in the fine grain fraction (< 2 microns). It constitutes the clay aggregate's main mineral phase and is easily observed either in thin sections or under SEM. This result indicates that smectite is the dominant mineral group in all layers.

TEM images reveal that in most cases, smectite is well crystallised as euhedral plates presenting a sub-hexagonal habitus (Fig. 2 A, B, E). The plates are not randomly distributed but organised geometrically, suggesting crystallisation from a solution such as those formed during synthesis experiments of smectite (Mosser-Ruck *et al.,* 1999) or micas (Barronnet *et al.,* 1976). Such growth corresponds to those described as issued from Ostwald ripening. The polygonal euhedral crystals are typical of clays formed from a solution and not resulting from the in situ alteration of a former silicate. They precipitated after the dissolution of Al, Si, and Mg bearing phases, which could be volcanic glass in the present cases.

Within the fine-grain fraction, smectite is generally mixed and associated with palygorskite, as shown by the images from Figure 6 (B, C, D). XRD spectra show that the analysed clay is fully expandable, probably montmorillonite, with a 001 reflection indicating a layer spacing of around 14 Å and swelling after glycolation around 17 Å. Results are almost similar for the 28 samples investigated, meaning that the nature of the smectite is identical, whatever the location and distribution within the different geological formations. The analyses show that the montmorillonite is silica-rich, with relatively low content in Mg and Fe, and the interlayer is dominated by K and Ca.

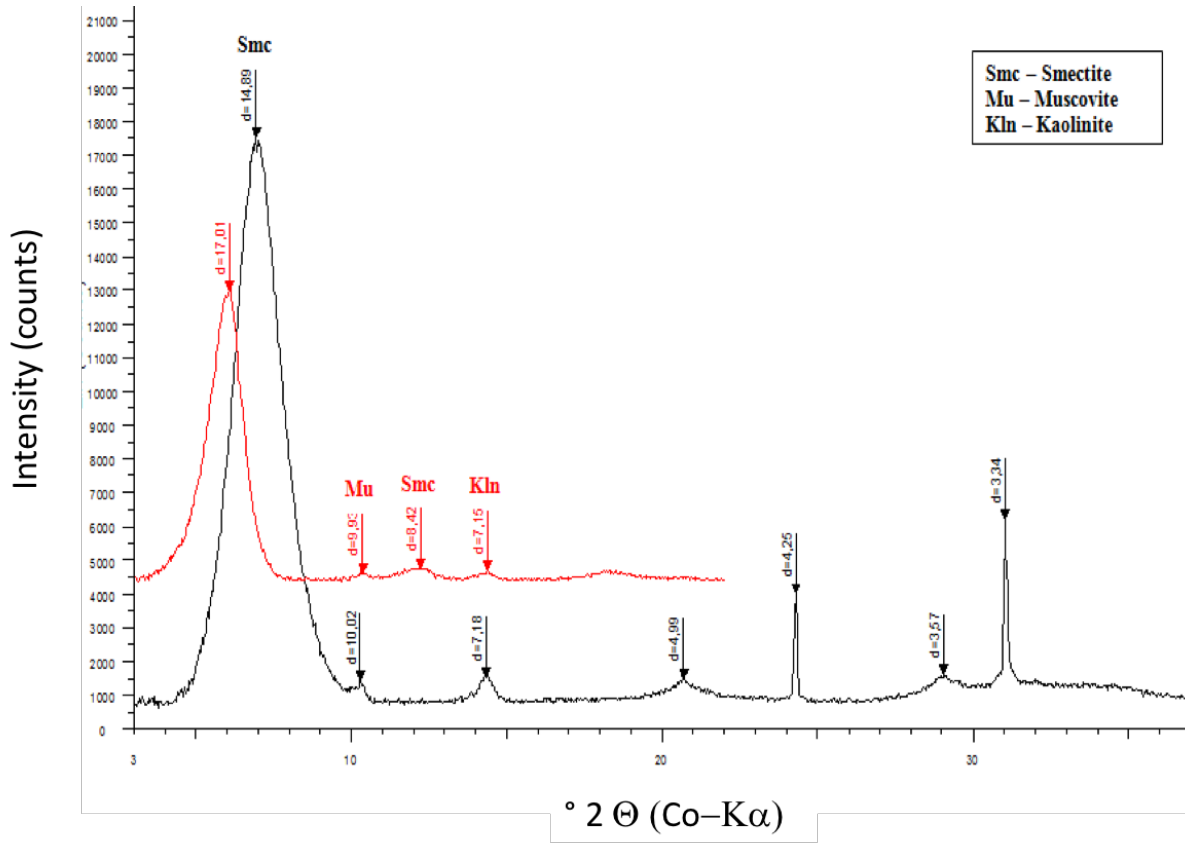

29 ***Figure 1. XRD pattern of the clay fraction from a representative South Muyunkum grey sand (sample 761-2)***

30

Sample	Horizon (Field)	Mineral	Si	Al(IV)	Al	Al(VI)	Fe3+	Mg	K	Na	Ca	C.I.
1750-45	Uyuk (TN)	Smectite	3,55	0,45	2,11	1,66	0,32	0,15	0,07	0,00	0,09	0,24
1750-48	Uyuk (TN)	Smectite	3,72	0,28	1,70	1,42	0,42	0,19	0,17	0,00	0,09	0,36
642-2	Uyuk (CM)	Smectite	3,74	0,26	1,72	1,46	0,38	0,20	0,10	0,00	0,11	0,32
761-2	Ikansk (SM)	Smectite	3,66	0,34	1,85	1,51	0,39	0,16	0,07	0,00	0,12	0,30
761-2	Ikansk (SM)	Smectite	3,71	0,29	1,87	1,58	0,29	0,18	0,04	0,00	0,14	0,32
761-2	Ikansk (SM)	Smectite	3,59	0,41	2,14	1,74	0,25	0,09	0,10	0,04	0,07	0,28
761-2	Ikansk (SM)	Smectite	3,71	0,29	1,81	1,52	0,40	0,13	0,04	0,00	0,12	0,27
761-2	Ikansk (SM)	Smectite	3,75	0,25	1,79	1,54	0,37	0,14	0,06	0,00	0,10	0,26
761-2	Ikansk (SM)	Smectite	3,72	0,28	1,81	1,53	0,35	0,18	0,05	0,00	0,10	0,26

761-2	Ikansk (SM)	Smectite	3,72	0,28	1,83	1,55	0,36	0,15	0,06	0,00	0,10	0,26
761-2	Ikansk (SM)	Smectite	3,51	0,49	2,25	1,76	0,23	0,10	0,16	0,00	0,07	0,31

Table 1: Representative analyses of the smectites from the sample 761-2

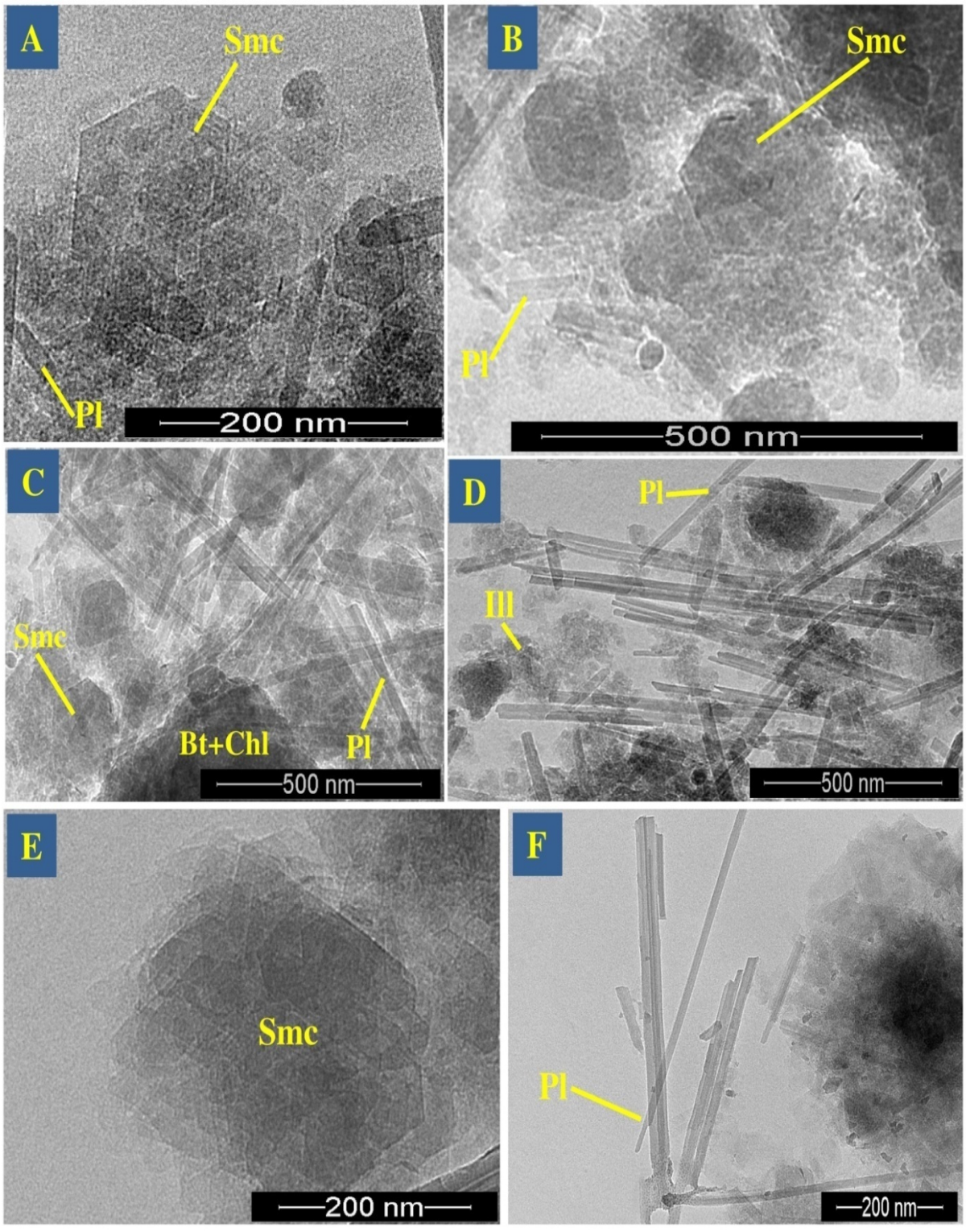

Figure 2. TEM microphotographs show the habitus of smectite with the geometric growth of euhedral crystals as formed by Ostwald ripening (A, B, E) and associated palygorskite (C, D, E). A-D: sample 1750-14; E: 1750-24; F: 421-5a, b.

Muscovite, Illite and mixed layered Illite-Smectite

Most sands and clay-rich layers contain muscovite, one of the main constituents of silici-clastic formations. Therefore, although the < 2-micron fraction has been separated, muscovite particles are almost always present.

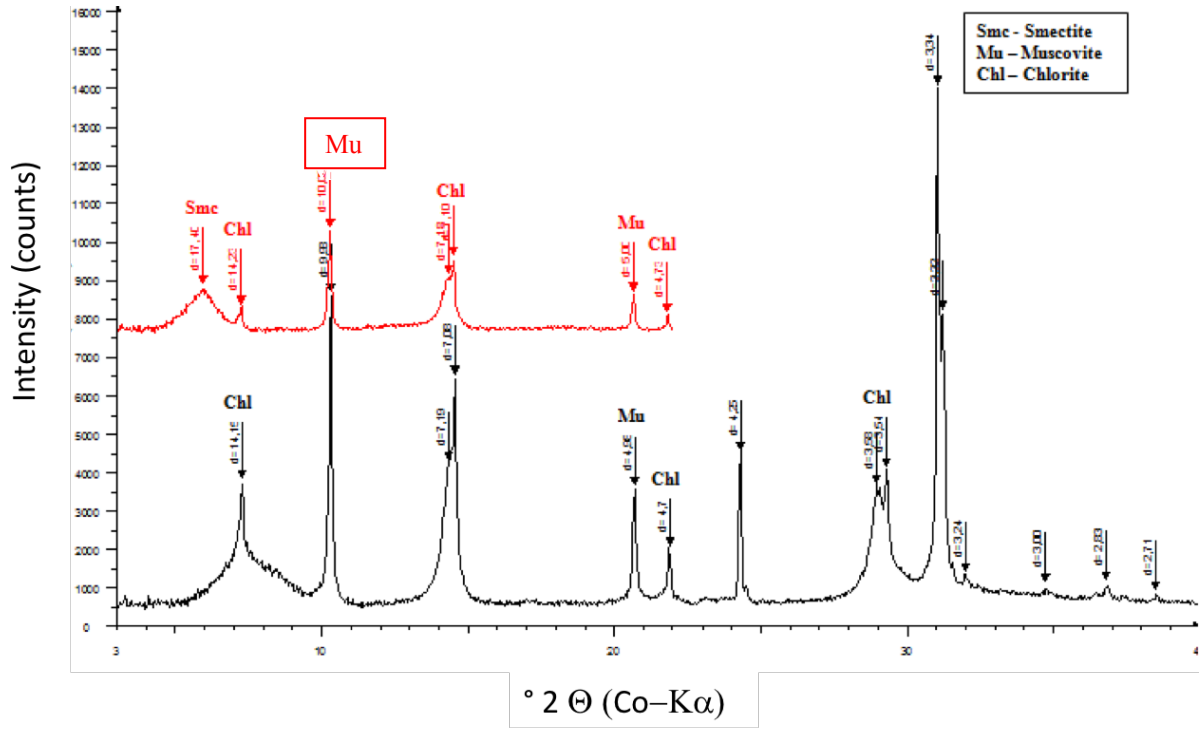

Figure 3. X-ray diffractogram (XRD) of the clay fraction from sample 996-10 dominated by detrital minerals: chlorite and muscovite

Sample	Horizon (Field)	Si	Al(IV)	Al	Al(VI)	Fe3+	Mg	K	Na	Ca	C.I.
774-1a,b	Ikansk (SM)	3,20	0,80	2,51	1,71	0,18	0,10	0,91	0,00	0,01	0,93
774-1a,b	Ikansk (SM)	3,24	0,76	2,42	1,66	0,20	0,09	0,85	0,03	0,01	0,89
996-10	Uyuk (CM)	3,06	0,94	2,71	1,78	0,17	0,05	0,99	0,00	0,00	0,99
996-10	Uyuk (CM)	3,10	0,90	2,76	1,86	0,02	0,11	0,84	0,11	0,00	0,95

Table 2: Structural formula of detrital muscovite calculated based on 11 oxygens.

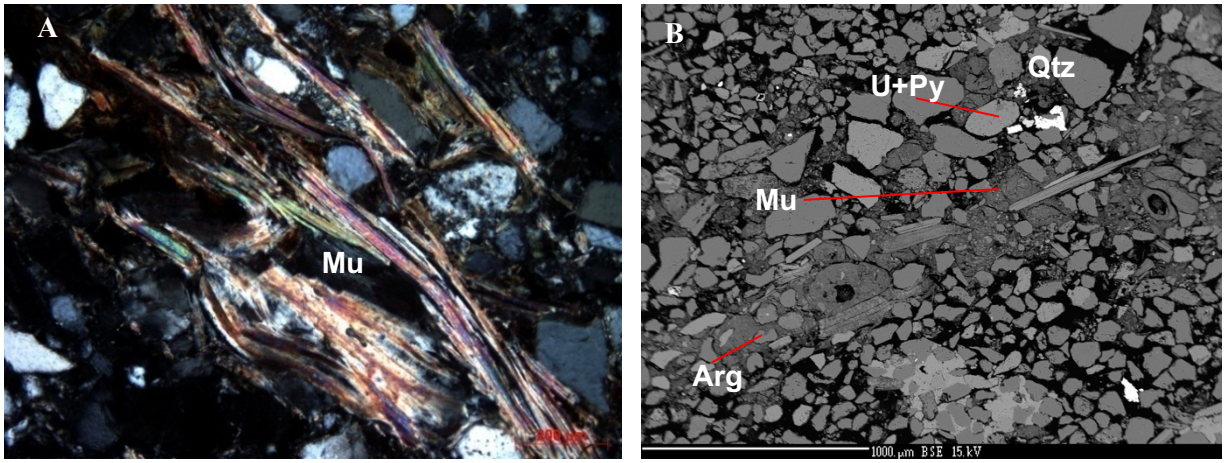

Figure 4. A: Detrital muscovite plates (crossNicholss, optical microscopy); B: backscattered SEM image showing a layer enriched in muscovite and clay in the sandstone. Arg: Clay; Fds: Feldspar; Mu: Muscovite; Py: Pyrite; Qtz: Quartz; U: Uranium phases (coffinite) associated with pyrite.

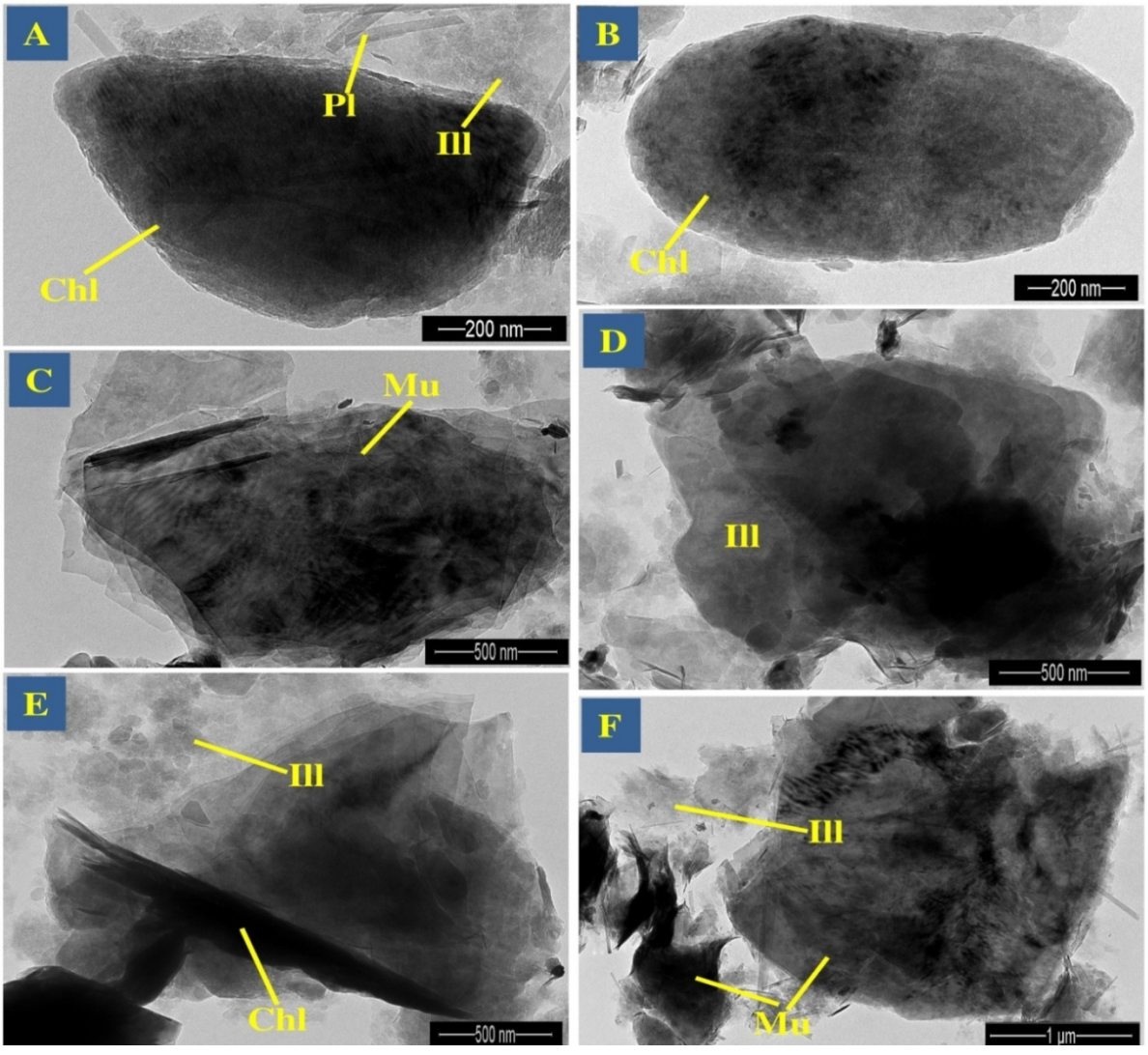

Figure 5. TEM microphotographs show the habitus of muscovite (C, F), illite (D, E) and chlorite (A, B).

Depending on their relative abundance, the muscovite particles are identified by a thin 001 reflection indicating the presence of di-octahedral phyllosilicates with a spacing of around 10 Å. It is, therefore, challenging to discriminate well-crystallised illite from small muscovite particles using XRD patterns. The two main criteria that can be used to differentiate illite and mixed layered illite-smectite from muscovite are the broadening of the 001 reflections on the XRD spectra and the chemical analyses, and structural formulae may reveal a deficiency in the interlayer site occupancy (table 3).

In the Uyuk formation, illite was found in Central Muyunkum and Tortkuduk. Within the Ikansk formation, illite is dominated only in South Muyunkum and is partially noticed in the samples of the Tortkuduk. Also, illite is uniformly represented in the Intymak and Betpakdala horizons all along the basin.

Sample	Horizon (Field)	Mineral	Si	Al(IV)	Al	Al(VI)	Fe3+	Mg	K	Na	Ca	C.I.
1321-70	Uyuk (TN)	Illite	3,28	0,72	2,61	1,90	0,05	0,07	0,74	0,00	0,00	0,75
1750-24	Uyuk (TN)	Illite	3,21	0,79	2,52	1,73	0,24	0,06	0,70	0,00	0,02	0,74
421-5 a,b	Uyuk (CM)	Illite	3,39	0,61	2,18	1,57	0,30	0,11	0,70	0,00	0,05	0,80
421-5 a,b	Uyuk (CM)	Illite	3,31	0,69	2,25	1,56	0,23	0,24	0,79	0,00	0,02	0,83
642-2	Uyuk (CM)	Illite	3,43	0,57	2,15	1,59	0,20	0,17	0,84	0,00	0,01	0,86
774-1a,b	Ikansk (SM)	Illite	3,37	0,63	2,37	1,73	0,15	0,11	0,74	0,00	0,01	0,75
774-1a,b	Ikansk (SM)	Illite	3,29	0,71	2,45	1,74	0,18	0,07	0,78	0,00	0,01	0,81
774-1a,b	Ikansk (SM)	Illite	3,12	0,88	2,58	1,70	0,23	0,07	0,89	0,05	0,02	0,97
774-1a,b	Ikansk (SM)	Illite	3,32	0,68	2,34	1,66	0,17	0,17	0,86	0,00	0,00	0,86
996-1	Intymak (CM)	Illite	3,58	0,42	1,97	1,55	0,17	0,26	0,71	0,00	0,01	0,72
996-10	Uyuk (CM)	Illite	3,27	0,73	2,30	1,57	0,33	0,14	0,71	0,00	0,01	0,72
996-10	Uyuk (CM)	Illite	3,12	0,88	2,73	1,85	0,16	0,00	0,78	0,05	0,01	0,86
996-10	Uyuk (CM)	Illite	3,31	0,69	2,30	1,61	0,24	0,11	0,89	0,00	0,01	0,92

Table 3. Structural formulas of illite calculated based on 11 oxygens.

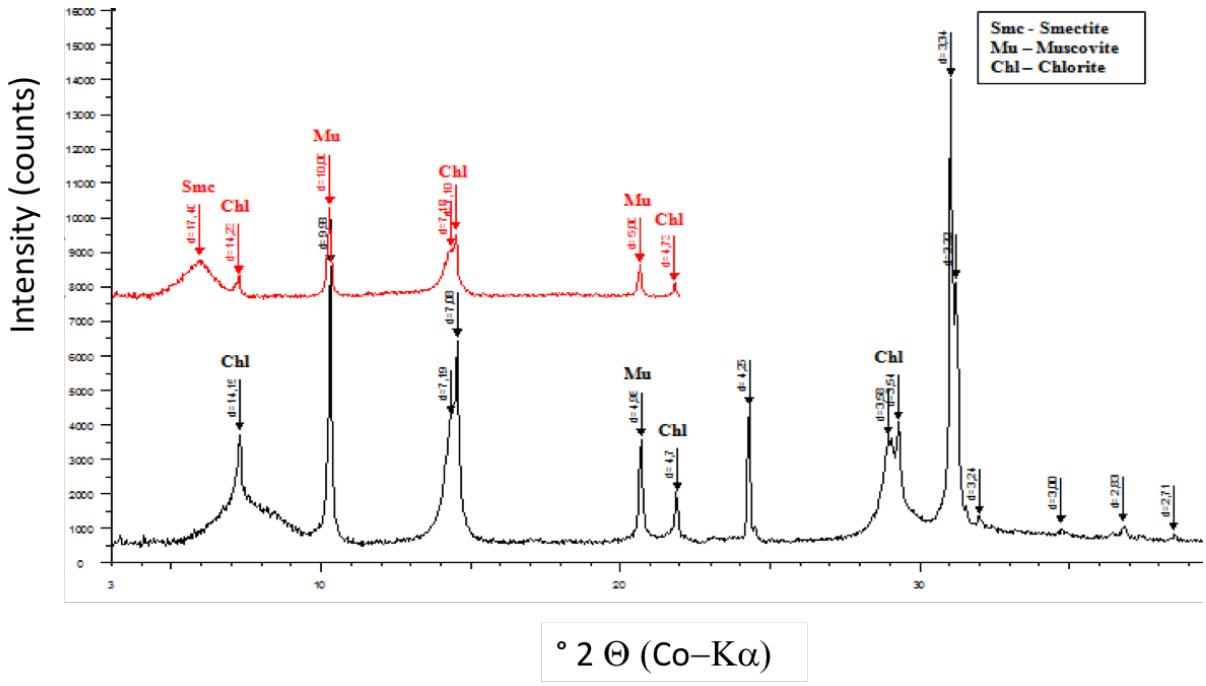

Figure 6. X-ray diffractogram of sample 996-10 from Central Muyunkum showing abundant well-crystallised K-micas (illite, muscovite) in addition to chlorite and smectite illite; a 2-micron fraction, black: air dried; red: glycolated).

Kaolinite

The kaolinite mineral group is much less frequent than smectite, the predominant fine-grain clay, and muscovite (illite) group. Kaolinite is present in small amounts as isolated particles as observed in thin sections but also under (TEM image, Fig. 6) and identified only in detectable amounts by XRD in a few samples. In the Tortkuduk field, it is noticed in the Intymak formation, whereas in the Central part of Muyunkum, kaolinite is present in both Uyuk and Intymak horizons.

A

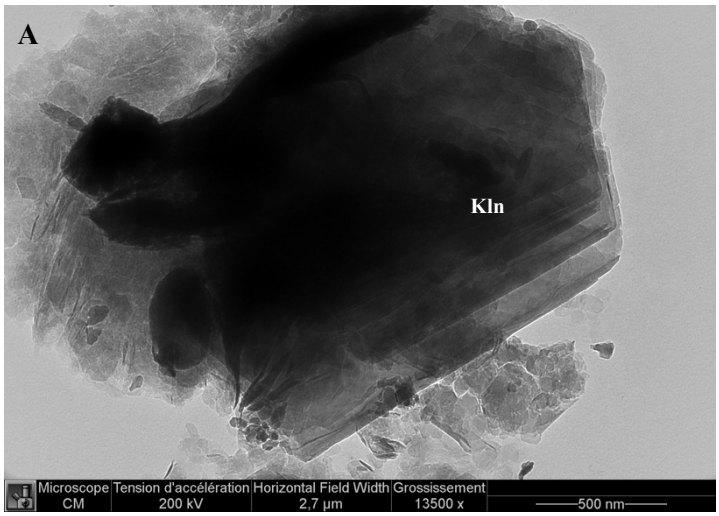

B

Element	Wt%
O	47.62
Na	0.00
Mg	0.02
Al	22.15
Si	25.54
K	0.40
Ca	0.28
Fe	3.98
Total	**100,00**

Figure 6. A: TEM image of kaolinite in sample 1321-70.; B: Chemical composition of kaolinite (TEM EDS analysis)

Halloysite

Halloysite is a mineral close to kaolinite in composition and structure which is characterised by its no platy habitus contrarily to kaolinite. It is rather difficult to distinguish from kaolinite by XRD as both minerals are in low amounts in the samples, and the main determination comes from TEM investigations. Images show rolled sheets containing only Al and Si in relative proportion typical of 7Å alumino-silicates of the kaolinite-halloysite group (Figure 7).

The structural formulae are close to that expected for Halloysite:

$Al_2Si_2O_5OH_4$, $2H_2O$

with some deficit in Al compensated by iron and a slight excess in measured silica.

$Al_{1,88\text{-}1,91}\ Fe_{0,03\text{-}0,05}\ Si_{2,02\text{-}2,08}\ O_5\ OH_4$, $2H_2O$.

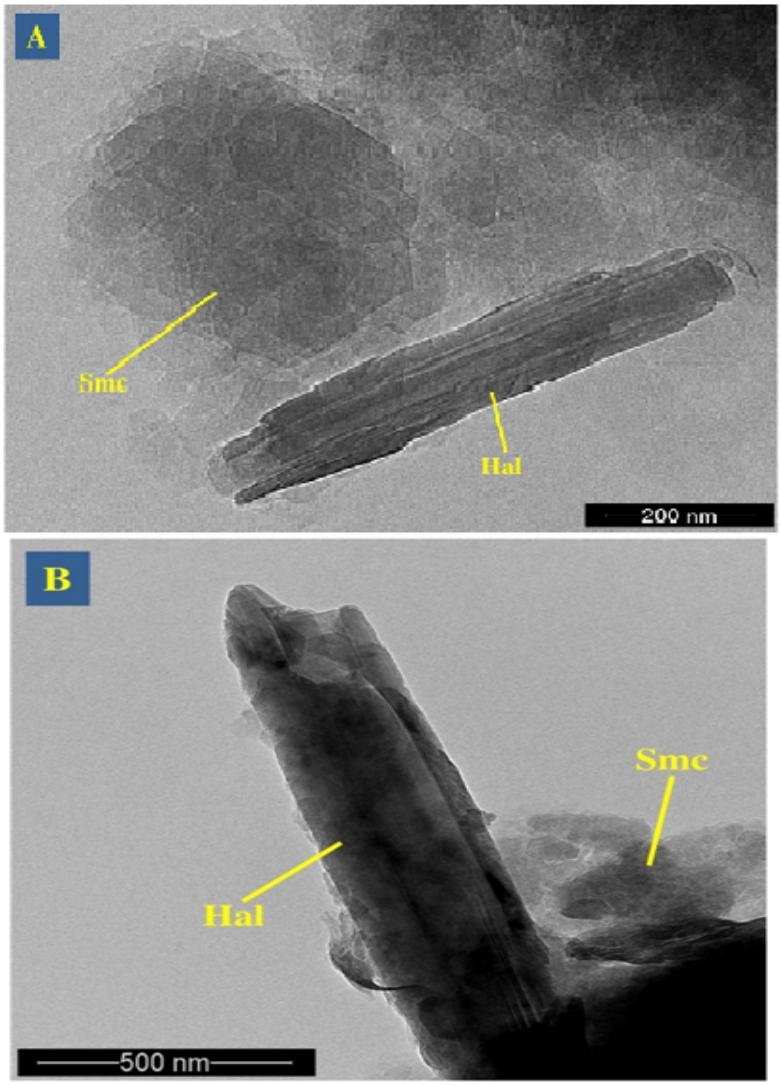

Figure 7. Habitus of halloysite in samples 1750-24 in A and 1750-24 in B (TEM image).

Palygorskite

Palygorskite is widely represented in the Tortkuduk field and selectively in other fields. If in Tortkuduk, the presence of palygorskite is almost omnipresent, then in Central and South Muyunkum, it is represented only in Intymak and Ikansk formations, respectively. It is generally intimately associated with smectite and identified by its typical reflections indicating a spacing of 10, 41 (43) Å on XRD spectra (Fig. 8). TEM images show that palygorskite forms long fibres, generally 500nm and up to a few microns, with a width of around 50±20 nm. It is tubular as chrysotile (Fig. 9).

Palygorskite (Mg, Al, vac)$_2$(Si$_{4-x}$, Al$_x$)$_4$ O$_{10}$(OH)$_4$-4H$_2$O is also characterised by its relatively high magnesium content (Table 4). The mean calculated structural formulas of analysed palygorskite are the following:

106 $(Mg_{0,86}Al_{0,94}\ vac_{0,2})_2(Si_{4,05})O_{10}(OH)_4\text{-}4H_2O$.

107

Sample	Horizon (Field)	Mineral	Si	Al(IV)	Al	Al(VI)	Fe3+	Mg	K	Na	Ca	C.I.
774-1a,b	Ikansk (SM)	Palygorskite	4,00	0,00	0,98	0,98	0,19	0,69	0,06	0,00	0,03	0,11
1750-2	Betpakdala (TN)	Polygorskite	3,89	0,11	1,35	1,24	0,18	0,38	0,01	0,00	0,04	0,09
1750-14	Ikansk (TN)	Polygorskite	3,79	0,21	1,25	1,03	0,29	0,52	0,17	0,00	0,05	0,26

108

109 ***Table 4: Structural formulae of palygorskite (sample 774-1)***

110

111

A

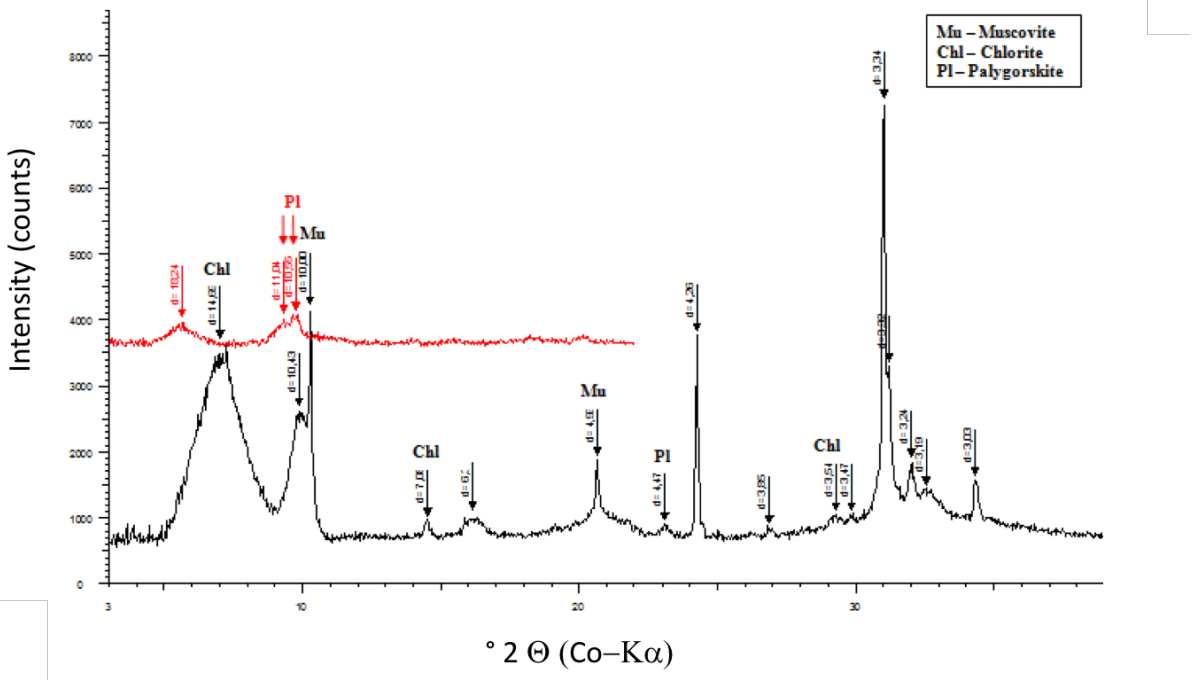

112

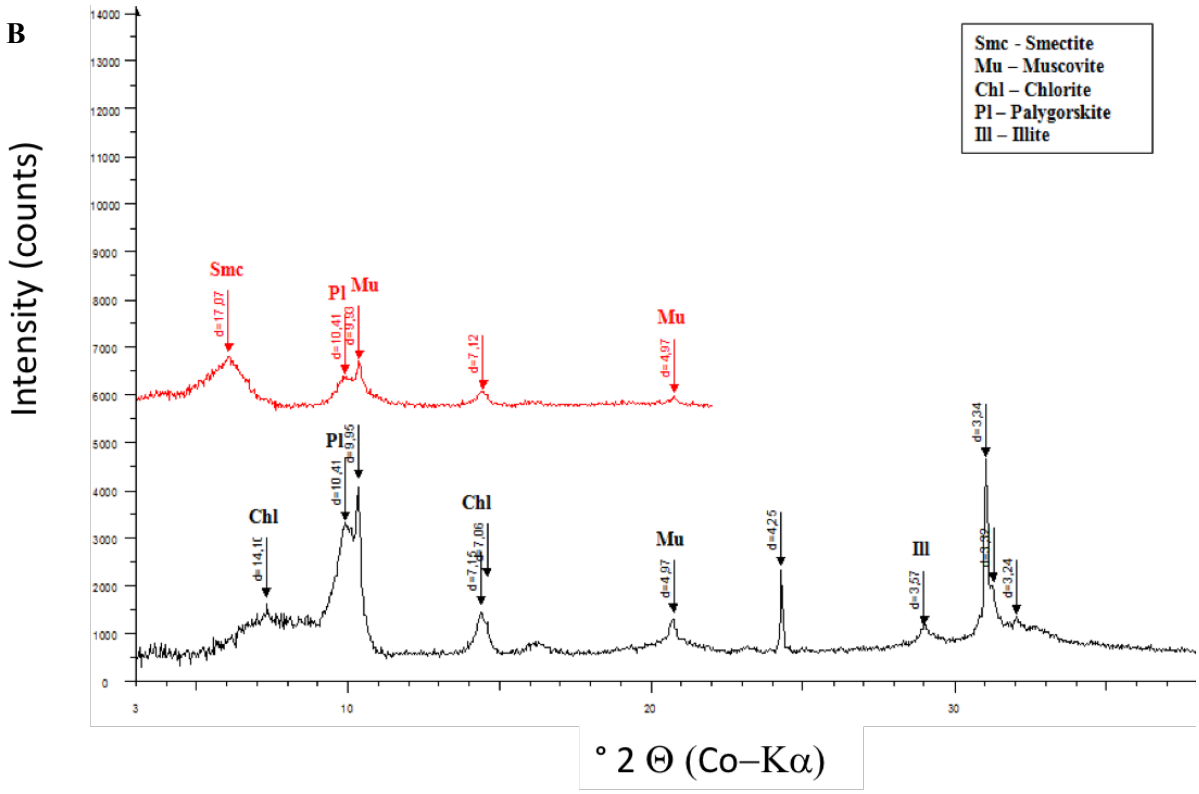

113

114 ***Figure 8. A: X-ray diffractogram of the samples 774-1a, b, and 1750-14. Palygorskite, like most other clays, is***
115 ***accompanied by smectites.***

116

117

118

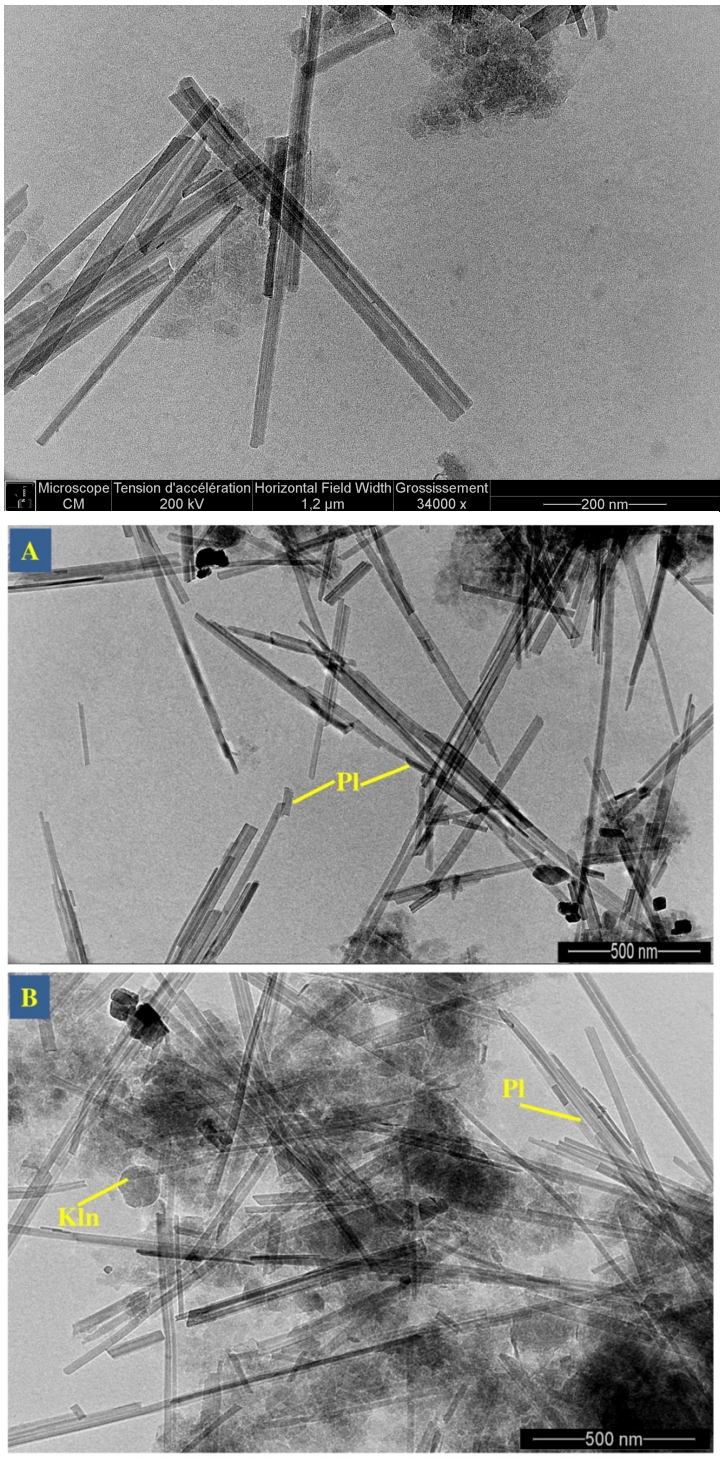

Figure 9. A: TEM microphotographs showing the habitus of palygorskite on the example of samples 774 and 1750-24.

Chlorite

"Chlorite" grains are mixtures of several minerals and could derive from the hydrothermal alteration of Fe-Mg-rich minerals such as biotite. The supergene alteration could have affected them during weathering and transport to the sediments. Therefore, an extensive range of

compositions is obtained from chlorite to mixtures with K-rich inherited material (altered biotite, mixing with illite etc.). As well as smectite and muscovite, chlorite is represented all along the studied horizons within the basin scale.

b- Crystal-chemical features of the analysed clays

The structural formula of the analysed clayey particles from 28 samples from the three fields (17 samples from Tortkuduk, 6 from Central Muyunkum and 5 from Southern Muyunkum) was considered. The data were obtained using TEM and Electron Microprobe analysis.

Figure x provides the main locations of reference minerals in a series of crystal-chemical diagrams showing the main di-and tri-octahedral clays. Structural formulas of the studied minerals for the diagrammatic interpretation were calculated concerning the oxygen 11 for di-octahedral clays and arbitrarily for the others to compare the whole populations. The main objective was to identify the main distribution of analytical data and composite particles, as clays are intimately associated. Microprobe and TEM data were used but presented in two different figures.

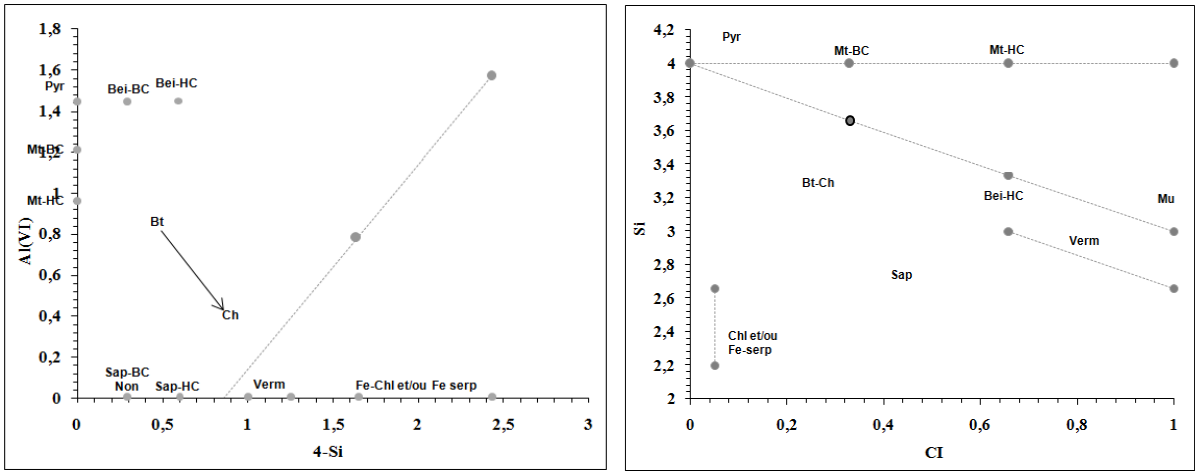

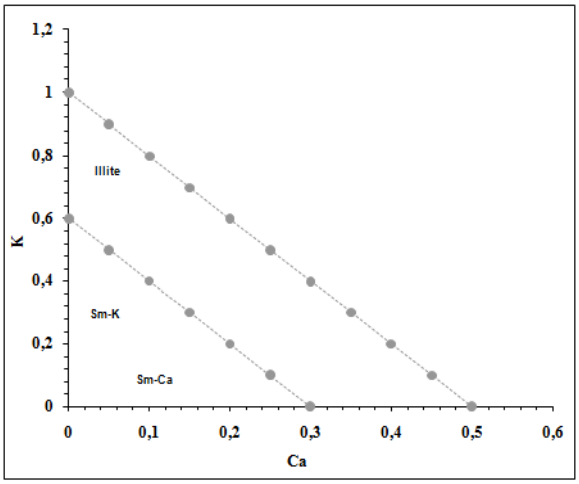

Figure 10. Diagrammatic of the crystal chemistry of clay minerals: Sm: Smectite; Bei: beidellite; Chl: chlorite; Mt: Montmorillonite, Mu: muscovite; Non: Nontronite; Pyr: Pyrophyllite; Sap: Saponite; Verm: Vermiculite, BC: low charge; HC: high charge; Al (VI) = AlTot-Al (IV) with Al (IV) = 4 -Si; Interlayer charge CI = Na + K +2 Ca.

145

146 The diagram, silica vs interlayer charge (I.C. $=Na^{+}+2Ca^{2+}+K^{+}$) diagram (Figure 11A) shows a
147 significant part of the analysed clays distributed in two populations: the smectite-I/S-illite-
148 muscovite trend in the field of di-octahedral clays and a second trend between the chlorite and
149 biotite-vermiculite crystal-chemical domains (when recalculated based on 11O). Thus, Fe-Mg
150 phases are characterised by lower Si content than di-octahedral series and plot below the line
151 delimiting the field of di-octahedral and tri-octahedral clays.

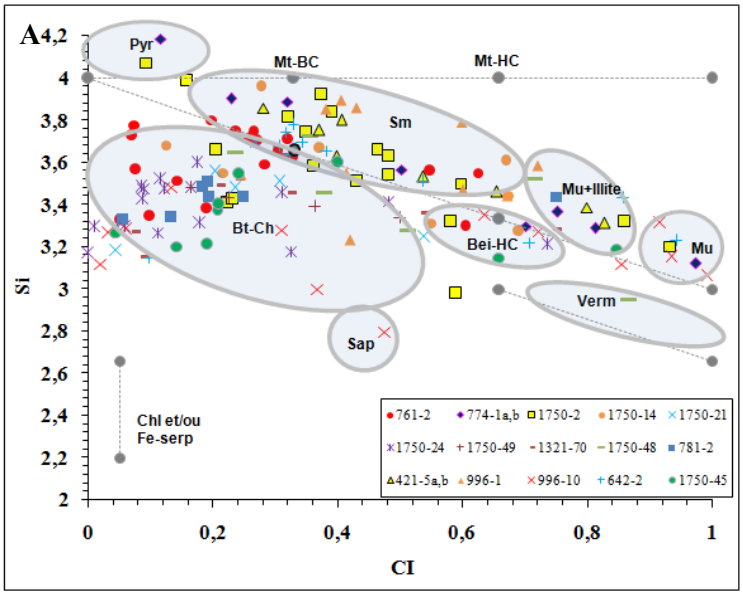

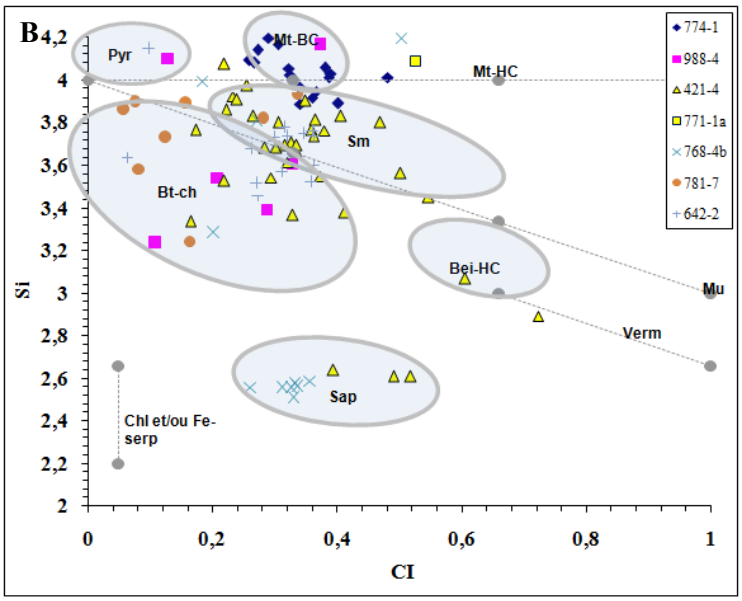

152 ***Figure 11. Si-interlayer charge diagram applied to TEM (A) and EMA analysis (B).***

153 Figure 11B show the two main crystal-chemical envelopes for large grains of detrital micas
154 and altered (chloritized) biotite. Micas are close to the muscovite end-member except for a few
155 points characterised by a lower interlayer charge. Most muscovites are well preserved in the
156 sands.

157 The biotite-chlorite assemblages display a large chemical envelope due to unachieved alteration
158 of the biotites, which includes both chlorites, as shown by XRD and TEM but also probably tri-
159 octahedral smectites.

160

161 *Diagram 4-Si – Al (IV)*

162 Most data plot within the smectite group field and between high-charge montmorillonite and
163 high-charge beidellite end-members. A few data correspond to low-charge beidellite, and some
164 composite particles fall between biotite and chlorite fields. A similar distribution is issued from
165 the EMA analysis (Figure 12). Both diagrams indicate that high-charge smectites dominate
166 most geological horizons.

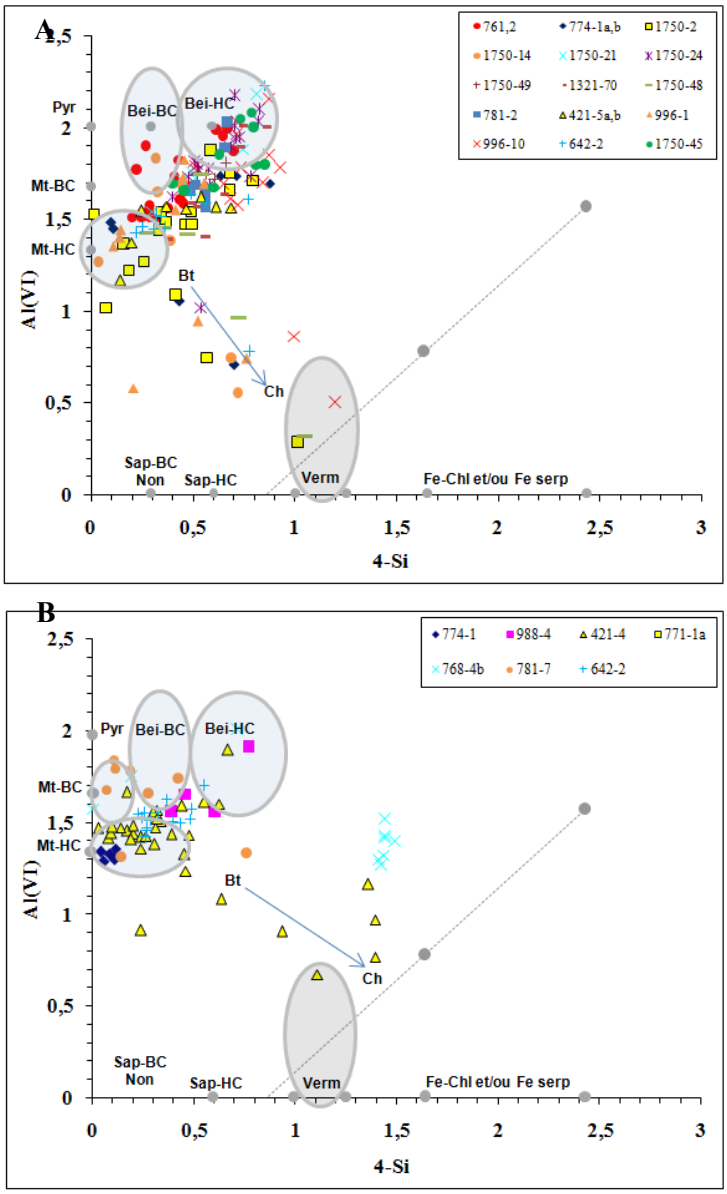

167 ***Figure 12. Diagram 4-Si –Al$^{(IV)}$ applied to A: TEM analyses and B: EMA analyses of clay particles.***

168

169 The K-Ca diagram (Fig. 13) discriminates K-rich di-octahedral micas such as muscovite and
170 illite and the smectites characterised by low charge (around 0,33) and an interlayer occupancy
171 by K, Ca (or Na).

172 Clays analysed by Electrom Microprobe are mostly smectites: the diagram shows they have a
173 mixed interlayer, dominated by K and Ca. Na is not presented and considered as it is only in
174 minor amounts. Clays analysed by TEM cover a larger range of compositions and include a few
175 illite and muscovite particles. The interlayer of the smectites is similar when analysed by both
176 techniques.

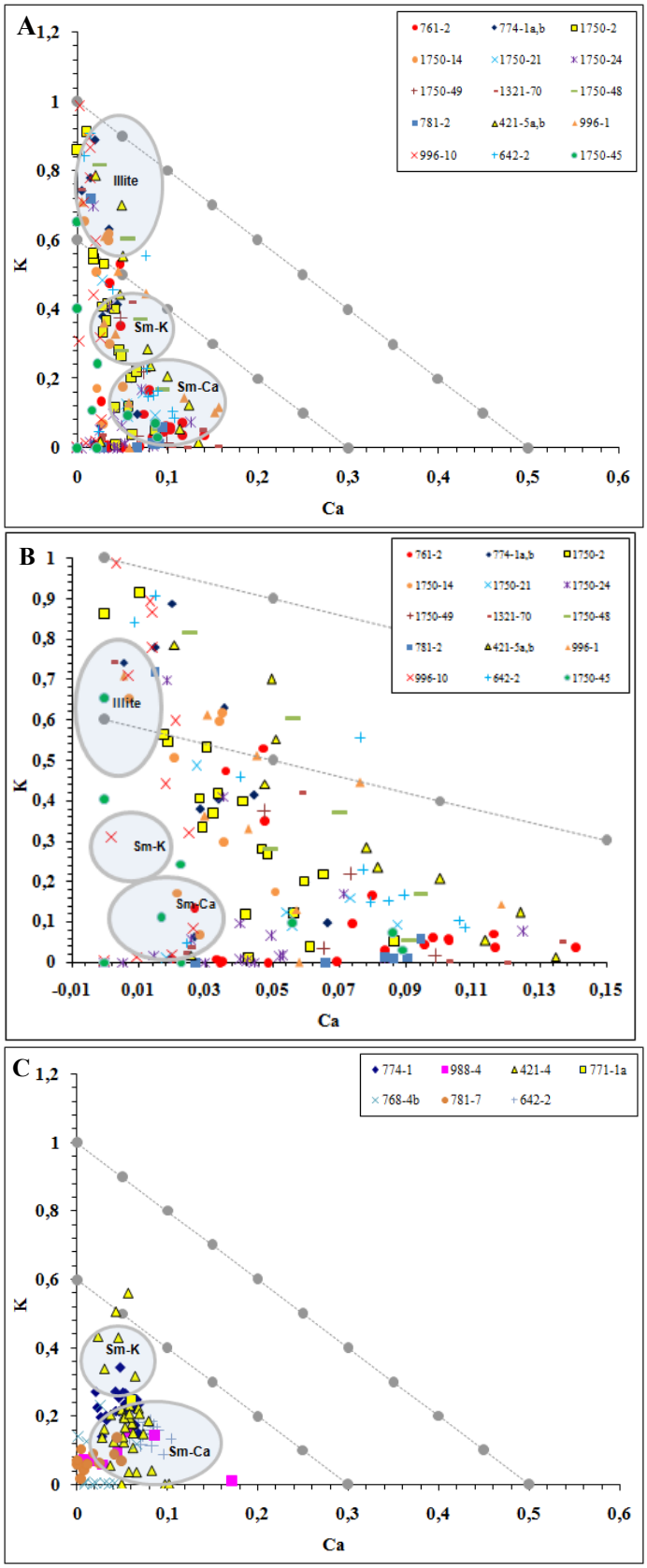

177 ***Figure 13. Ca – K diagram applied to data series obtained by TEM and microprobe analyses A: dioctahedral***
178 ***particles analysed by TEM; B: Enlarged part of Figure A; C: clay fraction analysed by EMA.***
179

4- Discussion

Samples from all localities and formations layers have a fine-grain clay fraction dominated by clays from the smectite group. Smectite composition falls in between high-charge montmorillonite and high-charge beidellite. The clay fraction also contains illite and particles of the chlorite-biotite group, besides the coarse grain fraction dominated by muscovite. Palygorskite was found in a significant number of samples in minor amounts detectable with TEM observations, but in some samples, palygorskite was detectable amounts with XRD. It is generally associated with smectite. In the Uyuk and Ikansk formations, other minerals such as halloysite, natrolite and albite were found, although in Betpakdala and Uyuk-Kyzylshy horizons, such minerals were not identified.

The association between smectite and palygorskite has been mentioned in a significant number of continental basins, generally characterised by:

- Alternated periods of dry and warm/humid periods, e.g. a marked seasonality, which could correspond to a subtropical climate;
- Alteration of volcanic glass, which facilitated the formation of clays from the solution enriched in alkalis, from Si and Al released during glass dissolution.

The formation of newly formed euhedral crystals of smectite is not so common. It may indicate a slow process of crystallisation from a solution oversaturated with respect to smectite, e.g. a solution saturated at less with respect to quartz and probably with amorphous silica, with a ratio, cation/H^+, sufficiently high to be out of the stability field of Al hydroxides and kaolinite (e.g. a pH enough high or a relatively high cation activity) but below the cation ratio favouring the formation of albite, analcime or natrolite. The fact that some traces of these minerals have been found in the smectite may indicate that locally the conditions were close to the smectite/Na-silicates boundary. Palygorskite may indicate that locally high Mg and Si content are reached in the interstitial fluids, maybe during dry periods.

It is difficult to determine whether smectite and palygorskite are synchronous and issued from the same process and element source, precipitated both or not from solutions or if they can result from authigenesis within the deposited sediment. This question has been frequently debated in the 1990's (Jones, 1986; Torres-Ruiz *et al.,* 1994). Thus, some authors consider that palygorskite results from direct saturation of the fluid with respect to palygorskite (Singer,

1979). Still, others think the mineral results from the replacement of another clay, such as smectite (Tazaki *et al.,* 1987).

The main question in the case of the Muyumkum area is to determine whether newly formed clays have been developed in situ in the sediments during sedimentation or transported along short distances from a lacustrine site, for instance. In all cases, the assemblage tends to indicate the formation of authigenic clays but in relation to surface paleoconditions and not in connection with the shallow burial of the sediments.

Such conditions are frequently reached in laterally extensive lakes formed after rainfall or swamp.

Some examples are listed below:

- Palygorskite, in palaeosols from the Miocene Xiacaowan Formation of Jiangsu and Anhui Provinces: Long *et al.* (1997) describe the occurrence of palygorskite (5 millions tons) and smectite as alteration products of basalts during the continental alteration of tertiary basalts near Nanjing (Jiangsu province, China) during a period of subtropical alteration;
- Tertiary continental basins in Spain, where sandstones and clay formations alternate, host Mg-rich clays, palygorskite, tri-octahedral smectite and sepiolite. These clays are considered authigenic and occur together, with illite and quartz being the only detrital phases. For the Madrid basin, Daams and Van de Meulen (1984) and Pozo and Casas (1997) proposed that these clays formed under arid to semiarid climatic conditions based on fossils and mineralogical assemblages;
- The occurrence of Mg–smectite, associated with minor sepiolite and palygorskite, has also been described in marine basins fed by clays formed in a lacustrine environment (Cavalcante *et al.* 2011). Notably, phosphate generally accompanies palygorskite and has also been found in great abundance, for instance, in sample 998-2. Jamoussi *et al.* (2003) have also described and discussed the occurrence of palygorskite in Tunisia and consider that it results from the transformation of previous silicates (smectites) which comes from close lacustrine type basin or playa-lake and accumulate in sediments during flooding episodes. The dissolution of the last smectite could result in palygosrskite precipitation, but this implies the loss of K and Al through a process of dissolution-precipitation in the presence of interstitial fluids enriched in magnesium and silica;

- In some basins, palygorskite is accompanied by smectite but in close association with dolocretes, as Colson et al. (1998) proposed for the formation of Danian formations in the Provence basin. This critical difference between the last case and the Kazakh basin, is the lack of calcretes or dolocretes. Clays formed, in the Provence basin, at the top of limestone reliefs, not from volcanites, and probably within a flood plain with a slope and relief different from the Kazakh paleorelief.

5- Conclusions

Newly formed smectite and palygorskite and their association are good proxies of a subtropical climate alternating dry and warm/ humid seasons during the late Cretaceous during the formation of the Chu-Syrasu basin. These clays may result partly from the alteration of volcanic rocks (glass) rather than from the alteration of the plagioclase of plutonic rocks. The association of fine grain clays, smectite and fibres (palygorskite) and the occurrence locally of grains of albite, and natrolite, indicate they formed from water, slightly alkali-rich, and enriched in silica and magnesium. Besides, muscovite as coarse grain particles, illite and chloritized biotites attest to a second source compatible with the coarse grain microcline and quartz, which can derive from granites.

Source rocks could be, therefore, acid plutonic series (peraluminous granites probably) releasing coarse-grained detrital phyllosilicates (muscovite and biotite-chlorite) and volcanic series, altered into newly-formed clays (smectite and palygorskite). It can be noticed that the preservation of euhedral newly-formed smectite is in favour of low temperature during early shallow burial as no evidence of significant mixed layering is detected. The K-Ca interlayer may attest to exchanges with the aquifer waters as the interlayer is expected to be more Na-rich in a playa lake or lacustrine environment.

Acknowledgements

This work was conducted within the framework of A. Munara's PhD thesis financed by a Bolashak grant (Ministery of Science and Education from Kazakhstan) and financial support from CREGU and Areva. J. Ghambaja is warmly thanked for his contribution to the TEM studies of clays.

References

Baronnet A., Amouric M. & Chabot B. (1976) Mécanismes de croissance, polytypisme et polymorphisme de la muscovite hydroxyl6e synth6tique. J. Cryst. Growth, 32, 37-59.

Bliachova S.M. et al. (1976). Paleontological and stratigraphic studies of Cretaceous, Paleogene and Neogene sediments of Chu-Sarysu depression, Report for the Meso-Cenozoic Part, 1972-75 yy. – Kokshetau, "Geoinform" (in Russian).

Bliachova S.M., Shakhverdov V.A. (1984). The partition and correlation of the Paleocene and Eocene of Chu-Sarysu depression. Moscow, Soviet geology, n° 2 (in Russian).

Cavalcante F., Belviso C., Bentivenga M., Fiore S., Prosser G. (2011) Occurrence of palygorskite and sepiolite in upper Paleocene–middle Eocene marine deep sediments of the Lagonegro Basin (Southern Apennines—Italy): Paleoenvironmental and provenance inferences, Sed. Geol., 233, 1–4, 1 42-52.

Colson, J., Cojan, I., Thiry M. (1998) A hydrological model for palygorskite formation in the Danian continental facies of the Provence Basin (France). Clay Min., 33, 333-347.

Daams R., van der Meulen A. (1984). Paleoenvironmental and paleoclimatic interpretation of micromammal faunal succession in the Upper Oligocene and Miocene of North Central Spain. Paleobiol. Cont. 14, 241-257.

Jamoussi, J. Ben Aboud, A., López-Galindo A. (2018). Palygorskite genesis through silicate transformation in Tunisia continental Eocene deposits. Clay Minerals 38, 2, 187–199.

Jones, B.F. (1986). Clay mineral diagenesis in lacustrine sediments. U.S. Geol. Surv. Bull., 1578: p. 291-300.

Long, D.G.F., McDonald A.M., Facheng Y., Houjei L., Zili Z., Xu T. (1997). Palygorskite, in palaeosols from the Miocene Xiacaowan Formation of Jiangsu and Anhui Provinces, P.R. China. Sed. Geol., 112, 3-4, 281-295.

Mosser-Ruck, R., Cathelineau, M., Baronnet, A., and Trouiller A. (1999) Hydrothermal reactivity of K-smectite at 300°C and 100 bar: dissolution-crystallisation process and non-expandable dehydrated smectite formation. Clay Min., Mineral Soc., 1999, 34 (2),.275-290.

Pozo M. and Casas J., (1999). Origin of kerolite and associated magnesium clays in palustrine-lacustrine environments. The Esquivias deposit (Neogene Madrid Basin, Spain). Clay Min., 34, 395-418.

Shakhverdov V.N., (1988). Metallogeny of uranium of Paleogene deposits of Chu-Sarysu province. Thesis St-Petersbourg, Vsegey. 24, p. 315-317.

Tazaki, K., Fyfe W.S., Tsuji M., Katayama, K. (1987) TEM observation of the smectite-to-palygorskite transition in deep Pacific sediments. Appl. Clay Sci., 2, 223-240.

Torres-Ruiz J., López-Galindo A., González-López J.M., Delgado A. (1994) Geochemistry of Spanish sepiolite-palygorskite deposits: Genetic considerations based on trace elements and isotopes. Chem. Geol., 112, 221-245.